Temporal Dynamics and Performance Association of the *Tetrasphaera*-Enriched Microbiome for Enhanced Biological Phosphorus Removal

Hui Wang[1,2,3], Yubo Wang[2,3], Guoqing Zhang[2], Ze Zhao[2], Feng Ju[2,3,4]*

[1] Environmental Science and Engineering Department, Zhejiang University, Hangzhou 310012, Zhejiang Province, China

[2] Key Laboratory of Coastal Environment and Resources of Zhejiang Province, School of Engineering, Westlake University, 18 Shilongshan Road, Hangzhou 310024, Zhejiang Province, China

[3] Institute of Advanced Technology, Westlake Institute for Advanced Study, 18 Shilongshan Road, Hangzhou 310024, China

[4] Center of Synthetic Biology and Integrated Bioengineering, School of Engineering, Westlake University, Hangzhou 310024 Zhejiang Province, China

*** Corresponding to:**

Dr. Feng Ju (Assistant Professor)

Address:

Environmental Microbiome and Biotechnology Lab (EMBLab)

Westlake University, 18 Shilongshan Road, Hangzhou 310024, China

Tel.: 571-87963205 (lab), 571-87380995 (office)

Fax: 0571-85271986

E-mail: jufeng@westlake.edu.cn

Abstract

Tetrasphaera were recently identified based on the 16S rRNA gene as among the most abundant polyphosphate-accumulating organisms (PAOs) in global full-scale wastewater treatment plants (WWTPs) with enhanced biological phosphorus removal (EBPR). However, it is unclear how *Tetrasphaera* PAOs are selectively enriched in the context of the EBPR microbiome. In this study, an EBPR microbiome enriched with *Tetrasphaera* (accounting for 40% of 16S sequences on day 113) was built using a top-down design approach featuring multicarbon sources and a low dosage of allylthiourea. The microbiome showed enhanced nutrient removal (P removal ~85% and N removal ~80%) and increased P recovery (up to 23.2 times) compared with the seeding activated sludge from a local full-scale WWTP. The supply of 1 mg/L allylthiourea promoted the coselection of *Tetrasphaera* PAOs and *Microlunatus* PAOs and sharply reduced the relative abundance of both ammonia oxidizer *Nitrosomonas* and putative competitors *Brevundimonas* and *Paracoccus*, facilitating the establishment of the EBPR microbiome. Based on 16S rRNA gene analysis, a putative novel PAO species, EBPR-ASV0001, was identified with *Tetrasphaera japonica* as its closest relative. This study provides new knowledge on the establishment of a *Tetrasphaera*-enriched microbiome facilitated by allylthiourea, which can be further exploited to guide future process upgrading and optimization to achieve and/or enhance simultaneous biological phosphorus and nitrogen removal from high-concentration wastewater.

Key words: Enhanced biological phosphorus removal (EBPR); Polyphosphate-accumulating organisms (PAOs); *Tetrasphaera*; Microbiome; Phosphorus recovery

1. Introduction

Phosphorus (P) eutrophication and P mineral resource depletion are increasingly serious global problems. Wastewater treatment plants (WWTPs) are both the sink and source for P [1, 2]. The bioprocess known as enhanced biological phosphorus removal (EBPR) can effectively promote P removal and recovery in WWTPs. It relies on a specific microbial functional guild called polyphosphate-accumulating organisms (PAOs) [3, 4]. Until now, most studies of EBPR microbiology have focused on *Ca.* Accumulibacter PAOs, which are commonly found in full-scale WWTPs and are widely enriched in lab-scale reactors using volatile fatty acids as carbon sources [4]. Because of the complex wastewater compositions and luxuriant growth conditions, full-scale WWTPs can provide diverse nutritional niches to accommodate various functional guilds [5, 6]. PAOs other than *Ca.* Accumulibacter (e.g., *Tetrasphaera* and *Dechloromonas*) are increasingly found to play an important but previously underappreciated role in full-scale systems [4, 7, 8], which encourages continued and follow-up efforts to explore the emerging aspects of the microbiology and ecology of the EBPR process.

Tetrasphaera PAOs have gained increasing attention due to their prevalence in global WWTPs as both important contributors to P removal and potential reservoirs for P recovery [4, 7]. For example, *Tetrasphaera* were found to be the most abundant PAOs in 18 Danish full-scale EBPR WWTPs [7] and were further revealed by Raman-FISH analysis to have a comparable or even higher P removal contribution than *Ca.* Accumulibacter PAOs [9]. In addition, *Tetrasphaera* PAOs are implicated in metabolizing various carbon sources (e.g., glucose and amino acids), which may favor their growth in WWTPs with fluctuating environmental conditions [10]. Although *Tetrasphaera* PAOs play an important role in the EBPR of full-scale WWTPs, how to selectively enrich and regulate them and how to enhance biological P removal (and thus recovery) remain elusive questions. Currently, *Tetrasphaera* PAOs, unlike the most

intensively investigated *Ca.* Accumulibacter, are still at an infancy stage of research. Our knowledge of the phylogeny, ecophysiology, and metabolism of *Tetrasphaera* PAOs, especially their capacity for wastewater P uptake and removal, is limited [4, 9, 10]. The successful isolation of six *Tetrasphaera* strains partially filled these knowledge gaps, but the physiologies and metabolic characteristics of these isolates in pure culture cannot explain the interactive behaviors of *Tetrasphaera* PAOs in WWTPs [11]. In addition, the high diversity and abundance of *Tetrasphaera* PAOs in EBPR plants generally imply the existence of yet-to-be-discovered PAOs. Therefore, it is essential to explore the enrichment method and microbial interactions of *Tetrasphaera* PAOs in the context of the EBPR microbiome.

Until now, only a few studies have reported *Tetrasphaera*-enriched microbiomes that were fed amino acids as a sole carbon source [10, 12-14]. The enrichment strategy, process, and key biotic and abiotic factors are unclear, hindering the in-depth study of the ecophysiology and metabolism of *Tetrasphaera* PAOs. Notably, allylthiourea ($C_4H_8N_2S$), a specific nitrification inhibitor, is empirically supplemented to facilitate the enrichment of model PAOs (mainly *Ca*. Accumulibacter) in lab-scale EBPR reactors by suppressing nitrite production by ammonia-oxidizing bacteria (AOB) to alleviate adverse competition from denitrifying bacteria [15, 16]. Because *Tetrasphaera* PAOs possess versatile metabolism, including the denitrifying capability, the effect of allylthiourea on enriching *Tetrasphaera* PAOs needs to be explored. Recently, a top-down approach has been proposed that uses intricately designed operation conditions (e.g., substrate composition, loading rate, and redox conditions) to manipulate an existing microbiome through ecological selection to perform the desired biological processes [17]. While this new methodological framework provides an ideal theoretical guide for the establishment of the *Tetrasphaera*-enriched microbiome, a practical strategy is lacking and needs to be established. Additionally, understanding of the microbiome dynamics and treatment performance during the *Tetrasphaera*-enriched

microbiome establishment process is lacking, especially regarding the influence of biotic and abiotic factors and the link to EBPR performance (i.e., P removal and recovery). This knowledge is the key to the reproducible establishment and precise regulation of a *Tetrasphaera*-enriched microbiome to improve EBPR performance.

Given the abovementioned knowledge gaps, our study aims to i) establish and explore a top-down strategy for *Tetrasphaera*-enriched microbiome establishment and characterize its P removal and recovery potentials, ii) investigate the microbiome temporal dynamics and interaction patterns of the *Tetrasphaera*-enriched microbiome establishment process, and iii) quantify the contribution of biotic and abiotic factors to microbiome dynamics and treatment performance. In addition, the nexus between microbial composition, environmental (e.g., operational) conditions, and treatment performance of the EBPR microbiome as well as the effect of allylthiourea on the enrichment of *Tetrasphaera* PAOs and EBPR performance have been investigated. To the best of our knowledge, this is the first proof-of-concept trial study to investigate the approaches and mechanisms of the establishment of the *Tetrasphaera*-enriched microbiome from its strategy design to the potential evaluation of P recovery.

2. Materials and Methods

2.1. Bioreactor setup and operation

To enrich *Tetrasphaera* PAOs, a lab-scale sequencing batch reactor with a working volume of 10 L was established and inoculated with activated sludge collected from a local municipal WWTP in Hangzhou, China. The WWTP employs the A/A/O process with $AlCl_3$ coagulating sedimentation in the primary setting tank, treating 50000 m^3/d of domestic wastewater. The 8-h cycle of reactor operation consisted of four phases: 150 min of anaerobic treatment, 320 min of aerobic treatment, 5 min of settling, and 5 min of water discharge and feeding. Operation details are provided in the

Supplementary Materials (Text S1).

2.2. Synthetic wastewater preparation and enrichment stages

The synthetic wastewater was prepared by mixing different volumes of stock solutions (A, B, C, and trace element solution, Table S1) to maintain a TOC concentration of 394.8 ± 34.7 mg/L, PO_4^{3-}-P concentration of 24.8 ± 3.9 mg/L, and NH_4^+-N concentration of 113.6 ± 36.9 mg/L. The characteristics of the prepared synthetic wastewater are similar to those of high-concentration wastewater (e.g., livestock wastewater [18]). Specifically, solution A (multicarbon sources) contained amicase (CAS No. 65072-00-6, Sigma–Aldrich), glucose (CAS No. 50-99-7, HuShi), and sodium acetate (CAS No. 127-09-3, HuShi). Solution B (P sources) contained K_2HPO_4 and KH_2PO_4. Solution C (mineral medium) contained NH_4Cl, $MgSO_4 \cdot 7H_2O$, and $CaCl_2 \cdot 2H_2O$. The trace element solution was prepared according to a previous study [15] and added to synthetic wastewater (1 mg/L). To investigate the effect of allylthiourea on *Tetrasphaera* PAOs enrichment and EBPR function, the entire reactor operation was divided into the following four stages with different dosages of allylthiourea:

- Stage I (day 0-73): In the natural enrichment phase, no allylthiourea (0 mg/L) was supplemented as a nitrification inhibitor.

- Stage II (day 74-120): In the reinforcement enrichment phase, allylthiourea was supplied at 1 mg/L to enhance the *Tetrasphaera*-related PAOs enrichment by partially inhibiting nitrification activity.

- Stage III (day 121-127): In the transient shock phase, the allylthiourea was added to 5 mg/L to strongly inhibit or suppress nitrification activity.

- Stage IV (day 128-170): In the recovery phase, the allylthiourea concentration was

adjusted back to 1 mg/L.

2.3. Batch experiments

Three batch tests were performed following experimental conditions similar to the mother reactor. Each test was seeded with the biomass collected from the EBPR reactor on day 143 when the relative abundance of *Tetrasphaera* sequences reached 30.3%. The composition of synthetic wastewater was consistent with Section 2.2 but only amended with three dosage levels of allylthiourea: 0 mg/L, 1 mg/L, and 5 mg/L. The pH and DO concentration were monitored using a portable multiparameter analyzer (HQ40d, Hach, USA). Seven samples were taken at three time points of the anaerobic phase (13, 45, and 135 min) and four time points of the aerobic phase (30, 90, 210, and 320 min). The sludge samples were centrifuged at 3000 rpm for 3 mins, and then the supernatant was collected for further physicochemical analysis.

2.4. Chemical analysis

The collected water samples were pretreated using 0.22 μm Millex GP syringe-driven filters to eliminate the potential solids before analysis. PO_4^{3-}-P, TN, and NH_4^+-N were analyzed using a segmented flow analyzer (San^{++}, SKALAR, Netherlands). The TOC was assessed by a TOC-L total organic carbon analyzer (Shimadzu, Japan). TS and VS were analyzed according to standard methods [19]. To evaluate the P recovery potential of the *Tetrasphaera*-enriched microbiome, the P weight percentage content in sludge ash was assessed and compared with the WWTP. Briefly, the sludge samples obtained from the *Tetrasphaera*-enriched reactor and local WWTP (the sampling site was the same as seeding sludge) were adjusted to the same TS content using pure water. Samples with a 50 mL volume were taken and put into a crucible for incineration (600 °C, 8 h). Then, the ash was collected and mixed using a mortar. The P weight percentage content in the sludge ash was assessed by a scanning electron microscope

170 equipped with an energy dispersive spectrometer (SEM–EDS) (Hitachi, Japan). Every
171 experiment was conducted with the triple treatments.

172 **2.5. FISH analysis of polyphosphate-accumulating organisms**

173 Fluorescence *in situ* hybridization (FISH) analysis was performed to investigate the
174 spatial organization of targeted PAOs in microbiome samples according to a previous
175 protocol with some modifications [20]. The detailed experimental flow and the
176 information of the FISH probes can be found in the Supplementary Materials (Text S2
177 and Table S2). FISH samples were observed using a laser scanning confocal microscope
178 (Zeiss, Zeiss LSM800, Germany).

179 **2.6. DNA extraction, PCR amplification, and sequencing**

180 Sludge samples were collected regularly at the end of the aerobic phase for DNA
181 extraction. A total of 16 samples were collected over 170 days. DNA extraction was
182 performed in duplicate from 1.5 ml collected reactor biomass using the Fast DNA SPIN
183 Kit for Soil (MP Biomedicals). The duplicate DNA extracts were mixed equally for
184 bacterial 16S rRNA gene high-throughput sequencing targeting the V1-V3
185 hypervariable regions (27 F: AGAGTTTGATCCTGGCTCAG and 534 R:
186 ATTACCGCGGCTGCTGG) [21] using Illumina's MiSeq platform with a paired-end
187 (2 × 300) sequencing strategy at Guangdong Magigene Biotechnology Co., Ltd., China.
188 The thermocycler (Bio-Rad S1000, Bio-Rad Laboratory) settings for PCR were initial
189 denaturation at 95 °C for 2 min, 30 cycles of 95 °C for 20 s, 56 °C for 30 s, and 72 °C
190 for 60 s, and final elongation at 72 °C for 5 min [21].

191 **2.7. Bioinformatics analysis**

192 Fastp was used to check the quality of the raw data with the sliding window parameter

of -W 4 -M 20. The primers were removed by using cutadapt software according to the primer information at the beginning and end of the sequence [22]. The obtained clean data were merged using QIIME2 (v. 2020.6) pipeline [23] with the DADA2 algorithm [24]. Briefly, the following steps were performed: i) filter out noisy sequences, ii) correct errors in marginal sequences, iii) remove chimeras sequence and singletons, iv) join denoised paired-end reads, and v) conduct sequence dereplication using a command of qiime dada2 denoise-paired with the parameter of --p-trunc-len-f 250 and --p-trunc-len-r 247 to maintain at least 12 bp overlap. The amplicon sequence variant (ASV) table was generated based on 100% sequence similarity for 16S rRNA genes, which contained 1389 ASVs in total. To exclude spurious sequences from the downstream analysis, the rare feature (i.e., ASV) with a total sequence count of less than 3 was removed using a command of qiime feature-table filter-features with the parameter of --p-min-frequency 3. To determine if the richness of the samples was fully sequenced, alpha rarefaction was analyzed using a command of qiime diversity alpha-rarefaction and visualized by the qiime 2 view website (https://view.qiime2.org/). A specific taxonomic classifier was trained based on the Silva_138.1_SSURef_NR99 database [25] and used for taxonomic analysis.

2.8. Phylogenetic analysis

The most abundant ASVs assigned to *Tetrasphaera* were selected to construct the phylogenetic tree using MEGA X [26]. Multiple sequence alignment was conducted by MUSCLE [27] with the default parameter. The evolutionary history was inferred by the maximum likelihood method and Kimura 2-parameter model. Two *Nitrosomonas europaea* sequences were used as the outgroup.

2.9. Statistical and network analysis

The statistical analyses, including redundancy analysis (RDA), principal coordinate

analysis (PCoA), Mantel test and PERMANOVA test, were performed using the R package vegan [28]. Co-occurrence networks were constructed using the 'Co-occurrence_network.R' script of package MbioAssy1.0 (https://github.com/emblab-westlake/MbioAssy1.0) [6, 29]. Detailed information on the co-occurrence network analysis is provided in the Supplementary Materials (Text S3). The network was visualized in Gephi 0.9.2 (https://gephi.org/).

3. Results and Discussion

3.1. The establishment strategy and performance of the *Tetrasphaera*-enriched microbiome

In this study, we established a strategy including four stages to selectively enrich *Tetrasphaera* PAOs based on the top-down design approach [17]. In stage I, the multicarbon sources (containing amicase, glucose, and sodium acetate) and periodic operational conditions (anaerobic/aerobic alternations) were designed as the selective tactics to conduct the initial enrichment. In stage II, 1 mg/L allylthiourea was introduced to facilitate enrichment by suppressing nitrification. In the following stages (stage III and IV), a transient shock with a high dosage of allylthiourea (5 mg/L) was applied to investigate the effect of allylthiourea dosage on the *Tetrasphaera*-enriched microbiome.

The treatment performance of nutrients (i.e., NH_4^+-N, TN, and PO_4^{3-}-P) and organic carbon (i.e., TOC) in wastewater followed over nearly six months (Fig. 1). In stage I, the reactor showed an overall decline in P removal efficiency (average 35%), but NH_4^+-N removal increased with prolonged operation (the highest NH_4^+-N removal was up to 92% on day 49). With the addition of allylthiourea (stage II), the efficiency of P removal significantly increased from 27.6% (day 73) to 86.2% (day 94) and then remained stable between 83.3% and 87.4%. The NH_4^+-N removal decreased significantly during day 73-90 (the lowest percentage was 3.9% on day 87) and then

243 recovered during day 105-121 (the average removal percentage was 97.6±3.0%). When
244 the concentration of allylthiourea was increased to 5 mg/L in stage III (transient shock
245 to suppress nitrification, Fig. 1C), the efficiency of P removal presented a slightly
246 decreasing trend (from 86.2% of day 122 to 73% of day 125), accompanying an obvious
247 decrease and final failure in NH_4^+-N removal. With the downregulation of the
248 allylthiourea level back to 1 mg/L on day 127 (stage IV), the efficiency of P removal
249 was recovered to the original level (67.4% to 89.3%), and the efficiency of TN removal
250 was stabilized at approximately 80% on day 148-170. In addition, the utilization and
251 degradation of organic carbon during the 170-day operation remained stable, and
252 approximately 95% of the carbon source could be absorbed and utilized (Fig. 1B).

253 In stage I, the noticeable increase in NH_4^+-N removal and general decrease in P
254 removal (between day 23 and day 46, see Fig. 1A against Fig. 1C) suggested an overall
255 negative relationship between nitrification and the P removal process. Considering the
256 high TN concentration in the effluent (Fig. 1D), the nitrification products (i.e., NO_2^- and
257 NO_3^-) may be accumulated, which could trigger the competition of denitrification for
258 the organic carbon source. Therefore, the nitrification process should be controlled to
259 promote PAO enrichment and enhance P removal. High P removal (85%) was achieved
260 in only 17 days upon adding 1 mg/L allylthiourea in stage II, indicating that the growth
261 and activity of PAOs were enhanced with the regulation of nitrification inhibitor.
262 Although the possibility could not be excluded that the increase in N removal in the late
263 phase of stage II could be partially attributed to the increase in the TOC/TN ratio (from
264 1.31 to 2.84), in stage IV, the TOC/TN ratio (2.90 ± 0.3) was stable, and both TN and
265 NH_4^+-N removal increased after the transient shock and were maintained in the late
266 phase. These results imply that the nitrification process of the microbial community
267 recovered, contributing to the increase in N removal. After the long-term selection
268 pressure of low dosage allylthiourea, the composition of the nitrifying bacteria in the
269 EBPR microbiome could be shifted, which agreed with a previous study in that

allylthiourea had an obvious effect on the structure of the nitrifying bacterial community [30].

3.2. The effect of allylthiourea on EBPR performance

To further investigate the effect of allylthiourea on the EBPR microbiome, batch experiments were conducted using 143-day microbiome biomass under different allylthiourea dosages (0 mg/L, 1 mg/L and 5 mg/L). Based on 16S rRNA gene amplicon sequencing analysis, the relative abundance of *Tetrasphaera* PAOs in the sampled 143-day EBPR microbiome was 30.3%. In addition, the corresponding removal efficiencies of PO_4^{3-}-P, TOC, NH_4^+-N, and TN in the mother EBPR reactor at 143 days were 91.9%, 97.9%, 92.3%, and 64.4%, respectively (Fig. 1). The P uptake rate with 1 mg/L allylthiourea addition was highest (0.07 mg/L·min), followed by 0 and 5 mg/L (0.04 and 0.05 mg/L·min, respectively) (Fig. 2A). In addition, the P removal efficiency in the 5 mg/L group was 67.9%, which was the lowest among the three groups (Fig. 2C). The NH_4^+-N profiles of the three groups were different, especially in the aerobic phase. NH_4^+-N removal did not occur under 5 mg/L allylthiourea, while a remarkable decline in NH_4^+-N concentration was observed with 0 mg/L and 1 mg/L allylthiourea. For example, the NH_4^+-N concentration decreased from 24.64 mg/L to 1.48 mg/L when 1 mg/L allylthiourea was added (Fig. 2B). In addition, the dynamics of dissolved oxygen (DO) showed no visible difference in the DO concentration among the three experimental groups in the anaerobic phase (< 0.2 mg/L), while in the following aerobic phase, the DO concentration increased to 5.21 mg/L at 53 mins when exposed to 5 mg/L allylthiourea (Fig. 2D). In comparison, the DO concentrations were 1.09 mg/L and 1.04 mg/L with allylthiourea concentrations of 0 mg/L and 1 mg/L, respectively.

With the dosages of 0 and 1 mg/L allylthiourea, the enriched microbial community achieved stable N and P removal. In contrast, the high allylthiourea dosage (5 mg/L)

showed a negative effect on the *Tetrasphaera*-enriched microbiome, consistent with the impact of allylthiourea addition on the nutrient removal performance previously observed in the EBPR reactor at stage III. The increased allylthiourea dosage (5 mg/L) inhibited the nitrification process, which could cause ammonia accumulation and disturbance in the microbial community [31]. In addition, when nitrification was completely inhibited, the production of NO_3^- and NO_2^- decreased, which may affect the activity and function of denitrifying PAOs. A previous study reported that although allylthiourea is soluble in water, it can be adsorbed by soil [30], indicating that allylthiourea may also be distributed in the sludge in addition to the aqueous phase. In addition, allylthiourea can be degraded by the microorganism; for example, a previous study indicated that 20 mg/L allylthiourea was degraded to 0.5–1.0 mg/L by activated sludge under aerobic conditions in 4 days [32], implying its low-security risk when applied for short-term biostimulation of wastewater treatment systems.

3.3. FISH analysis of the *Tetrasphaera*-enriched microbiome and evaluation of P recovery potential

The *Tetrasphaera*-enriched microbiome on day 143 was visualized by FISH. The targeted *Ca.* Accumulibacter and *Tetrasphaera* PAOs were visually detected in both the activated sludge sample (A) collected from the same WWTP as the seeding sludge (on December 2nd, 2020) and the *Tetrasphaera*-enriched microbiome (B) in our EBPR reactor (Fig. 3). Overall, *Tetrasphaera* PAOs were morphologically dominant in the EBPR microbiome, indicating that they were successfully enriched by the top-down design approach employed. Furthermore, the P storage ability and recovery potential of the *Tetrasphaera*-enriched microbiome were evaluated by determining the P content in the sludge ash using SEM–EDS. The P content (counted as the weight percentage) in *Tetrasphaera*-enriched sludge ash and secondary sink sludge ash was 32.5% and 1.4%, respectively. Therefore, the percentage of P in *Tetrasphaera*-enriched microbiome

321 sludge ash dramatically increased by 23.2 times compared with the normal full-scale
322 WWTP sludge, indicating that the P-storage ability of the *Tetrasphaera*-enriched
323 microbiome was largely enhanced. A strong signal intensity of Na and Mg elements
324 was detected in the *Tetrasphaera*-enriched sludge, while the Al and Si signal intensities
325 were higher in WWTP sludge (Fig. 3C). These results corresponded with the surface
326 morphology of these two kinds of sludge (Fig. 3A and Fig. 3B). The WWTP sludge ash
327 showed a red color with a loose structure because the WWTP influent contained sand,
328 and the WWTP used Al-based coagulants to aid nutrient removal from wastewater. In
329 comparison, the *Tetrasphaera*-enriched sludge ash showed a white color and compact
330 morphology, which resulted from the designed operation process and influent
331 compositions (e.g., $MgSO_4$ and $CaCl_2$). Theoretically, *Tetrasphaera*-enriched sludge
332 ash is attractive for further use in white P recovery and is promising to replace the
333 depleting phosphate rock, in which $Ca_3(PO_4)_2$ is the main component [33]. Therefore,
334 three essential conditions to promote P recovery from wastewater are achieved: i) high
335 P removal efficiency, ii) microbiome with enhanced P storage ability, and iii) P-rich
336 ashes and compounds for further value-added P recovery. The establishment of the
337 *Tetrasphaera*-enriched microbiome holds promise for exploiting *Tetrasphaera*
338 microbiology and EBPR biotechnology for the targeted regulation and promotion of
339 biological P recovery in full-scale WWTPs.

340 **3.4. The microbiome composition and dynamics during the establishment process**
341 **of the *Tetrasphaera*-enriched microbiome**

342 The microbiome composition and temporal dynamics during the enrichment process of
343 *Tetrasphaera* PAOs were investigated based on high-throughput 16S rRNA gene
344 amplicon sequencing (Fig. 4). In general, the microbiome was dominated by
345 *Tetrasphaera* PAOs in coexistence with *Microlunatus* PAOs and glycogen
346 accumulating organisms (GAOs) (i.e., *Ca.* Competibacter). In seed sludge,

347 *Tetrasphaera* PAOs, *Microlunatus* PAOs, *Brevundimonas*, and *Ca.* Competibacter
348 GAOs showed relative abundance of 1.5%, 0.1%, 0.3% and 12.4%, respectively. For
349 the initial establishment of the EBPR microbiome, their relative abundance on day 73
350 shifted to 13.5%, 2.3%, 15.1%, and 3.0%, respectively. In addition, the highest relative
351 abundance of *Tetrasphaera* PAOs was approximately 40% on day 113, approximately
352 equivalent to a cell or biovolume percentage of 62% to 67% by assuming an average
353 16S rRNA gene copy number of 1.0 for *Tetrasphaera* and between 2.5 and 3.0 for
354 activated sludge bacteria [34]. This result implied that allylthiourea promoted
355 significant enrichment of *Tetrasphaera* PAOs (*P value* = 0.017, Kruskal-Wallis test, Fig.
356 S1A). Notably, the *Tetrasphaera* PAOs were the most abundant 16S rRNA gene ASV
357 in the EBPR microbiome (i.e., EBPR-ASV0001). Phylogenetic analysis showed that
358 *Tetrasphaera sp.* EBPR-ASV0001 was phylogenetically different from the six
359 previously reported isolates (Fig. 4B and Table S3). The global similarity of 16S rRNA
360 gene sequences between EBPR-ASV0001 and *Tetrasphaera japonica* was 96.8%,
361 indicating that EBPR-ASV0001 is most likely a denitrifying PAO similar to *T. japonica*.

362 The abundance fluctuations of *Ca.* Competibacter GAOs, *Brevundimonas*, and
363 *Tetrasphaera* PAOs during stage I (day 0-73, Fig. 4A) were consistent with unstable
364 biological phosphorus and nitrogen removal. Specifically, *Ca.* Competibacter GAOs
365 decreased significantly in the first 33 days (*P value*=0.05, Kruskal-Wallis test), while
366 *Brevundimonas* and *Paracoccus* were markedly enriched during days 49-73 (*P*
367 *value*=0.05, Kruskal-Wallis test) (Fig. S1B, C, and D). In addition, the decrease in the
368 relative abundance of *Tetrasphaera* PAOs and the P removal efficiency coincided with
369 the prosperity of *Brevundimonas* and *Paracoccus*. Previous reports indicated that the
370 occurrence of the denitrification process in the anaerobic phase could cause EBPR
371 failure because some denitrifiers could compete for organics with PAOs [16].
372 *Brevundimonas* and *Paracoccus* are well known not only as denitrifiers but also as
373 heterotrophic nitrification and aerobic denitrification (HN-AD) bacteria, which can

374 simultaneously perform nitrification and denitrification under aerobic conditions [35-
375 37]. Therefore, their abundance increase could lead to potential competition for organic
376 molecules and/other resources with *Tetrasphaera* PAOs, especially in full-scale
377 WWTPs where the dissolved oxygen is heterogeneous.

378 With the addition of 1 mg/L allylthiourea, the following gradual abundance
379 increase in *Tetrasphaera* PAOs (13.0% to 37.7%) was coupled with the sharp
380 abundance decrease in *Nitrosomonas* AOBs (0.35% to 0.02%) as well as the denitrifiers
381 *Brevundimonas* (19.9% to 6.9%) and *Paracoccus* (5.8% to 1.1%) from day 66 (stage I)
382 to day 113 (stage II). This result can be explained by the chain effects associated with
383 the allylthiourea inhibition of nitrifying *Nitrosomonas*, i.e., the inhibition of autotrophic
384 ammonia oxidation largely reduced denitrifying substrates available to the dentritrifers,
385 thus greatly alleviating their competition against PAOs for organic resources (Fig. 4A).
386 Interestingly, the ammonia oxidizer *Nitrosomonas* decreased by 13.7 times from days
387 73 to 113 and disappeared on day 121, while high ammonia removal was still observed
388 (e.g., 98.7% on day 121, Fig. 1C), implying the existence of an alternative nitrification
389 process. We speculated that some heterotrophic nitrifiers should participate in the
390 nitrification process when autotrophic nitrifiers (e.g., *Nitrosomonas*) are evidently
391 inhibited under a low dosage of allylthiourea (i.e., 1 mg/L), facilitating the nitrogen
392 removal. In stage III, when the transient shock of 5 mg/L allylthiourea was applied,
393 PAOs fluctuated in their relative abundance, which first decreased to 12.6% on day 147
394 and then increased to 28.2% on day 157. We hypothesized that a high allylthiourea
395 dosage would adversely affect the proliferation and function of denitrifying PAOs that
396 can couple nitrate and/or nitrite reduction to P uptake due to the heavy suppression of
397 nitrification. Supporting this hypothesis, ammonia removal was completely suppressed
398 in stage III, accompanying a dramatic decline in the removal efficiency of TN and PO_4^{3-}
399 -P to 19.5% and 58.4%, respectively (Fig. 1A). Furthermore, a high allylthiourea dosage
400 restrained the propagation of the most abundant PAOs, *Tetrasphaera* sp. EBPR-

ASV0001, which showed a marked decline on day 142 (22.64%, Fig. 1B). Further genome-based study and laboratory isolation of *Tetrasphaera* sp. EBPR-ASV0001 to reveal its metabolic pathways, physiology, and application potential in full-scale EBPR WWTPs are warranted.

3.5. The microbial co-occurrence patterns during the establishment process of the *Tetrasphaera*-enriched microbiome

To predict microbial interactions in the *Tetrasphaera*-enriched microbiome, microbial co-occurrence patterns over the 170-day reactor operation were analyzed based on network analysis (Fig. 5). The positive bacterial association network had 85 nodes (ASVs) and 167 edges (correlations, Table S4), which were topologically partitioned into nine modules presumably representing discrete and interactive ecological niches over time (Fig. 5A). The topological properties of the observed network were calculated and compared with those of identically sized Erdös-Réyni random networks (Table S4). The clustering coefficient (CC) and modularity index of the observed *Tetrasphaera*-enriched co-occurrence network were 0.449 and 0.687 and higher than those of the corresponding Erdös-Réyni random networks (0.046 and 0.418), suggesting that the microbiome assembly process is nonrandom (or deterministic). Moreover, the network of the *Tetrasphaera*-enriched microbiome showed small-world properties with a coefficient ($\sigma = \frac{\gamma}{\lambda} = \frac{CC/CC_{random}}{APL/APL_{random}}$) [38] of 8.97, suggesting that the enrichment strategy adjusts the overall microbial interconnections and interior interaction relationship.

To link ecological niches of co-occurring taxa to their functionality, each network node was taxonomically assigned to three functional groups (Fig. 5B), according to previous reports [7, 29, 36, 39], including PAOs, GAOs, and nitrogen-removing bacteria (e.g., denitrifiers and HN-AD bacteria). Overall, *Tetrasphaera* was distributed

426 in four modules of the network (i.e., module II, IV, V, and VIII), implying niche
427 differences between members of the genus *Tetrasphaera*. This observation supported
428 the previous conclusion [4, 10, 12-14], namely, the different species of *Tetrasphaera*
429 could have a specific metabolic preference; therefore, the genus *Tetrasphaera* was
430 extremely versatile and could widely interact with coexisting bacteria in EBPR. In
431 particular, *Tetrasphaera* PAOs significantly co-occurred with *Microlunatus* PAOs in
432 module II (Spearman's ρ =0.906, FDR-adjusted $P < 0.01$, Fig. 5), indicating their
433 potential cooperative relationships. In addition, known denitrifiers (e.g.,
434 *Hyphomicrobium, Bosea*, and *Xanthobacter*) occurred with GAOs (e.g., *Ca.*
435 Competibacter, *Kineosphaera*, and *Micropruina*) in modules I, II and IV, implying a
436 shared niche preference, such as taking up organic matter for growth. The wide within-
437 module co-occurrence between denitrifiers and organic-degrading bacteria (e.g.,
438 *Hyphomicrobium* and *Shinella* in module I, *Bosea* and *TM7a* in module II, and
439 *Xanthobacter* and *Amaricoccus* in module IV) supports the classical presumption of
440 their cooperative interactions, such as cross-feeding, i.e., the former provides small
441 organic molecules for the latter as a carbon source.

442 The microbial interaction and niche patterns revealed in the co-occurrence network
443 of the *Tetrasphaera*-enriched microbiome (Fig. 5) were associated with the dynamics
444 of the removal efficiency of nutrients (A, C, and D) rather than organic carbon (B, Fig.
445 1). First, the wide co-occurrence and prevalence of denitrifiers and organic-degrading
446 bacteria in the same modules, together with the near-perfect TOC removal (95±1.2%)
447 and mostly favorable TN removal (77±2.9% when no inhibition occurred), implies that
448 chemoorganotrophic respiration and heterotrophic denitrification could be active
449 during the microbiome assembly process. Moreover, *Micropruina* was a fermentative
450 GAO [4], and its positive correlations with *Brevundimonas* in module V (Spearman's ρ
451 = 0.816) and *Paracoccus* in module IV (Spearman's ρ = 0.818) indicated the
452 fermentative bacteria may cross-feed co-occurring HN-AD bacteria with fermentation

453 products. Likewise, a positive correlation between *Tetrasphaera* PAOs and *Bosea*
454 denitrifiers (Spearman's ρ = 0.910, Fig. 5) suggests that denitrifying phosphorus
455 removal should have occurred in the reactor, promoting simultaneous biological N and
456 P removal. A prior genomic survey indicated that *Tetrasphaera* can utilize nitrite for
457 poly-P production [11], which could explain the abovementioned enrichment scenarios
458 of *Tetrasphaera* PAOs facilitated by cross-feeding partnerships with nitrate denitrifiers.
459 Therefore, the enrichment strategy with intricately designed multicarbon sources and
460 low-dose allylthiourea creates microbial niches and fosters diverse cooperative
461 interactions that affect the microbiome composition and establishment.

462 **3.6. The nexus between microbiome, environment, and EBPR performance**

463 In addition to microbiome dynamics and co-occurrence patterns, the roles of abiotic
464 factors (i.e., environmental condition and influent composition) and biotic factors (i.e.,
465 microbiome composition and interaction) in driving *Tetrasphaera*-enriched
466 microbiome establishment were explored based on RDA and PCoA analyses. The
467 microbial communities shifted away upon reactor startup and quickly assembled with
468 the continuous feedings of synthetic wastewater containing multicarbon sources (S1,
469 Fig. 6, and Fig. S2). When the nitrification inhibitor (i.e., allylthiourea) was introduced,
470 the microbial community was significantly selected and restructured (S2, S3, and S4,
471 Fig. 6 and Table S5). The nexus between the environmental condition and microbial
472 community was visualized with the first two RDA axes (Fig. 6A), which jointly
473 explained 52.2% of the total microbiome variances and indicated that the designed
474 environmental parameters, especially the inhibitor (adjusted $R^2 = 0.23$, *P value* < 0.01,
475 Table S6), were among the major drivers of the microbiome assembly process. In
476 addition, the *Tetrasphaera* PAOs and *Microlunatus* PAOs positively correlated with
477 allylthiourea and PO_4^{3-}-P, indicating that *Tetrasphaera* PAOs and *Microlunatus* PAOs
478 have growth advantages under selective conditions. The association analysis between

the microbial community and EBPR performance showed that *Tetrasphaera* PAOs, *Microlunatus* PAOs, and *Saccharimonadales* positively correlated with PO_4^{3-}-P, TN, and TOC removal. Meanwhile, *Brevundimonas* and *Kineosphaera* were positively correlated with NH_4^+-N removal (Fig. 6B). Consistent with the RDA results, Mantel test analysis revealed that allylthiourea significantly affected the microbiome dynamics and PO_4^{3-}-P removal (*P value* < 0.005, Table S7).

Overall, the correlation nexus between microbial (M) community, environmental (E) variables, and EBPR performance (P) (defined here as the 'MEP nexus') indicated that 1 mg/L allylthiourea, as a key abiotic factor, promoted the selection and proliferation of *Tetrasphaera* PAOs, *Microlunatus* PAOs and organic degrading bacteria *Saccharimonadales* while inhibiting *Nitrosomonas* AOBs and indirectly affecting potential competitors such as denitrifying *Brevundimonas*. Furthermore, the removal of carbon and nutrients (i.e., TOC, TN, and PO_4^{3-}-P) was enhanced. Notably, *Tetrasphaera* and *Microlunatus* PAOs showed no significant negative correlation in their relative abundance in the whole process (Fig. S3), and their positive co-occurrence patterns (Module II, Fig. 5A) made their coexistence feasible in the *Tetrasphaera*-enriched EBPR microbiome. In addition, *Saccharimonadales* is reported to be a key degrader of organic molecules (e.g., glucose and sugars) in aerobic sludge systems [40]. Based on their temporal dynamics, *Microlunatus* PAOs and *Saccharimonadales* should be the key biotic factors that benefit from the designed multicarbon sources and positively contribute to building a *Tetrasphaera*-enriched microbiome and enhancing the reactor performance for organics and P removal. In summary, the MEP nexus indicates that the enrichment strategy designed here has realized the selective enrichment of *Tetrasphaera* PAOs as an outcome of co-actions from both abiotic and biotic factors.

4. Conclusion

In this study, an enrichment strategy featuring intricately designed multicarbon sources amended with low dosage allylthiourea was proposed and applied to build a *Tetrasphaera*-enriched EBPR microbiome. Based on 16S rRNA gene amplicon sequencing analysis, a novel putative *Tetrasphaera* PAO species, EBPR-ASV0001, was identified and enriched at a relative abundance of 40%. The established microbiome showed enhanced P removal (~85%) and N removal (~80%) and a 23.2 times higher P content in the sludge ash than in the normal full-scale WWTP sludge. The addition of low-dosage allylthiourea (e.g., 1 mg/L demonstrated in this study) regulated the community structure and affected the microbial co-occurrence patterns, which can be advised as a short-term biostimulation approach for the quick selection and enrichment of *Tetrasphaera* PAOs to strengthen biological P removal. The findings of this study expand our knowledge of the temporal dynamics and interaction patterns of a novel putative PAO member of *Tetrasphaera*. Future studies with metagenomic analysis or full-length 16S rRNA sequencing of the enriched *Tetrasphaera* species are needed to verify their phylogeny and putative function more reliably as new PAOs. Nonetheless, from an engineering perspective, this outcome provides theoretical guidance for exploiting and optimizing EBPR application for sustainable P removal and recovery coupled with biological nitrogen removal from high-concentration wastewater.

Acknowledgement

This work was supported by the Key R&D Program of Zhejiang (2022C03075), Zhejiang Provincial Natural Science Foundation of China under Grant No. LR22D010001. We would like to thank Dr. Xiao Yang and Dr. Xiangyu Yang for the helpful discussion and technical advice. The author would like to thank Yisong Xu for her professional support in equipment procurement and lab management. We thank the

Microscopy Core Facility of Westlake University for the facility support and thank technician Fang Xiao for technical assistance. We thank the Research Center for Industries of the Future (RCIF), the Instrumentation and Service Center for Molecular Sciences and Physical Sciences, and The Westlake University-Muyuan Group Joint Research Institute at Westlake University for support. We thank the Westlake University HPC Center for computation support.

Data availability

The raw data of 16S rRNA gene amplicon sequencing were deposited in China National GeneBank (CNGB) under the project accession number CNP0002991.

Conflict of Interests

The authors declare no conflict of interests.

References

[1] Deletic A, Wang H. Water Pollution Control for Sustainable Development. Engineering 2019;5(5):839-840.

[2] Soares A. Wastewater treatment in 2050: Challenges ahead and future vision in a European context. Environ Sci Ecotechnology 2020;2:100030.

[3] Garcia Martin H, Ivanova N, Kunin V, Warnecke F, Barry KW, McHardy AC, Yeates C, He S, Salamov AA, Szeto E, Dalin E, Putnam NH, Shapiro HJ, Pangilinan JL, Rigoutsos I, Kyrpides NC, Blackall LL, McMahon KD, Hugenholtz P. Metagenomic analysis of two enhanced biological phosphorus removal (EBPR) sludge communities. Nat Biotechnol 2006;24(10):1263-1269.

[4] Nielsen PH, McIlroy SJ, Albertsen M, Nierychlo M. Re-evaluating the microbiology of the enhanced biological phosphorus removal process. Curr Opin Biotechnol 2019;57:111-118.

[5] Ju F, Zhang T. Advances in meta-omics research on activated sludge microbial community. Microbiology China 2019;46(2038):14.

[6] Ju F, Zhang T. Bacterial assembly and temporal dynamics in activated sludge of a full-scale municipal wastewater treatment plant. ISME J 2015;9(3):683-695.

[7] Stokholm-Bjerregaard M, McIlroy SJ, Nierychlo M, Karst SM, Albertsen M, Nielsen PH. A Critical Assessment of the Microorganisms Proposed to be Important to Enhanced Biological Phosphorus Removal in Full-Scale Wastewater Treatment Systems. Front Microbiol 2017;8:718.

[8] Petriglieri F, Singleton C, Peces M, Petersen JF, Nierychlo M, Nielsen PH. "Candidatus Dechloromonas phosphoritropha" and "Ca. D. phosphorivorans", novel polyphosphate accumulating organisms abundant in wastewater treatment systems. ISME J 2021;15(12):3605-3614.

[9] Fernando EY, McIlroy SJ, Nierychlo M, Herbst FA, Petriglieri F, Schmid MC, Wagner M, Nielsen JL, Nielsen PH. Resolving the individual contribution of key microbial populations to enhanced biological phosphorus removal with Raman-FISH. ISME J 2019;13(8):1933-1946.

[10] Liu R, Hao X, Chen Q, Li J. Research advances of Tetrasphaera in enhanced biological phosphorus removal: A review. Water Res 2019;166:115003.

[11] Kristiansen R, Nguyen HT, Saunders AM, Nielsen JL, Wimmer R, Le VQ, McIlroy SJ, Petrovski S, Seviour RJ, Calteau A, Nielsen KL, Nielsen PH. A metabolic model for members of the genus Tetrasphaera involved in enhanced biological phosphorus

removal. ISME J 2013;7(3):543-554.

[12] Marques R, Ribera-Guardia A, Santos J, Carvalho G, Reis MAM, Pijuan M, Oehmen A. Denitrifying capabilities of Tetrasphaera and their contribution towards nitrous oxide production in enhanced biological phosphorus removal processes. Water Res 2018;137:262-272.

[13] Marques R, Santos J, Nguyen H, Carvalho G, Noronha JP, Nielsen PH, Reis MAM, Oehmen A. Metabolism and ecological niche of Tetrasphaera and Ca. Accumulibacter in enhanced biological phosphorus removal. Water Res 2017;122:159-171.

[14] Close K, Marques R, Carvalho VCF, Freitas EB, Reis MAM, Carvalho G, Oehmen A. The storage compounds associated with Tetrasphaera PAO metabolism and the relationship between diversity and P removal. Water Res 2021;204:117621.

[15] Lu H, Oehmen A, Virdis B, Keller J, Yuan Z. Obtaining highly enriched cultures of Candidatus Accumulibacter phosphates through alternating carbon sources. Water Res 2006;40(20):3838-3848.

[16] Guerrero J, Guisasola A, Baeza JA. The nature of the carbon source rules the competition between PAO and denitrifiers in systems for simultaneous biological nitrogen and phosphorus removal. Water Res 2011;45(16):4793-4802.

[17] Lawson CE, Harcombe WR, Hatzenpichler R, Lindemann SR, Loffler FE, O'Malley MA, Garcia Martin H, Pfleger BF, Raskin L, Venturelli OS, Weissbrodt DG, Noguera DR, McMahon KD. Common principles and best practices for engineering microbiomes. Nat Rev Microbiol 2019;17(12):725-741.

[18] Hu H, Li X, Wu S, Yang C. Sustainable livestock wastewater treatment via phytoremediation: Current status and future perspectives. Bioresour. Technol. 2020;315:123809.

[19] SEPA, State Environmental Protection Administration of China (SEPA) Monitoring and Analysis Methods of Water and Wastewater, China Environmental Science Press, Beijing, 2002.

[20] Roots P, Wang Y, Rosenthal AF, Griffin JS, Sabba F, Petrovich M, Yang F, Kozak JA, Zhang H, Wells GF. Comammox Nitrospira are the dominant ammonia oxidizers in a mainstream low dissolved oxygen nitrification reactor. Water Res 2019;157:396-405.

[21] Albertsen M, Karst SM, Ziegler AS, Kirkegaard RH, Nielsen PH. Back to Basics--The Influence of DNA Extraction and Primer Choice on Phylogenetic Analysis of Activated Sludge Communities. PLoS One 2015;10(7):e0132783.

[22] Martin M. Cutadapt removes adapter sequences from high-throughput sequencing reads. EMBnet. journal 2011;17(1):3.

[23] Bolyen E, Rideout JR, Dillon MR, Bokulich NA, Abnet CC, et al.. Reproducible, interactive, scalable and extensible microbiome data science using QIIME 2. Nat Biotechnol 2019;37(8):852-857.

[24] Callahan BJ, McMurdie PJ, Rosen MJ, Han AW, Johnson AJ, Holmes SP. DADA2: High-resolution sample inference from Illumina amplicon data. Nat Methods 2016;13(7):581-583.

[25] Quast C, Pruesse E, Yilmaz P, Gerken J, Schweer T, Yarza P, Peplies J, Glockner FO. The SILVA ribosomal RNA gene database project: improved data processing and web-based tools. Nucleic Acids Res 2012;41(D1):D590-596.

[26] Kumar S, Stecher G, Li M, Knyaz C, Tamura K. MEGA X: Molecular Evolutionary Genetics Analysis across Computing Platforms. Mol Biol Evol 2018;35(6):1547-1549.

[27] Edgar RC. MUSCLE: multiple sequence alignment with high accuracy and high throughput. Nucleic Acids Res 2004;32(5):1792-1797.

[28] Team RC. R: A language and environment for statistical computing. 2013.

[29] Ju F, Xia Y, Guo F, Wang Z, Zhang T. Taxonomic relatedness shapes bacterial assembly in activated sludge of globally distributed wastewater treatment plants. Environ Microbiol 2014;16(8):2421-2432.

[30] Wang YF, Gu JD. Effects of allylthiourea, salinity, and pH on ammonia/ammonium-oxidizing prokaryotes in mangrove sediment incubated in laboratory microcosms. Appl Microbiol Biotechnol. 2014;98(7):3257-3274.

[31] Vadivelu VM, Keller J, Yuan Z. Effect of free ammonia on the respiration and growth processes of an enriched Nitrobacter culture. Water Res 2007;41(4):826-834.

[32] Liu B, Terashima M, Quan NT, Ha NT, Van Chieu L, Goel R, Yasui H. Determination of optimal dose of allylthiourea (ATU) for the batch respirometric test of activated sludge. Water Sci Technol 2018;77(11-12):2876-2885.

[33] Yang X, Nohira T. A New Concept for Producing White Phosphorus: Electrolysis of Dissolved Phosphate in Molten Chloride. ACS Sustainable Chem Eng 2020;8(36):13784-13792.

[34] Ju F, Beck K, Yin X, Maccagnan A, McArdell CS, Singer HP, Johnson DR, Zhang T, Burgmann H. Wastewater treatment plant resistomes are shaped by bacterial composition, genetic exchange, and upregulated expression in the effluent microbiomes. ISME J 2019;13(2):346-360.

[35] Tan X, Yang YL, Li X, Zhou ZW, Liu CJ, Liu YW, Yin WC, Fan XY. Intensified nitrogen removal by heterotrophic nitrification aerobic denitrification bacteria in two

pilot-scale tidal flow constructed wetlands: Influence of influent C/N ratios and tidal strategies. Bioresour Technol 2020;302:122803.

[36] Song T, Zhang X, Li J, Wu X, Feng H, Dong W. A review of research progress of heterotrophic nitrification and aerobic denitrification microorganisms (HNADMs). Sci Total Environ 2021;801:149319.

[37] Zhu Z, Yang Y, Fang A, Lou Y, Xie G, Ren N, Xing D. Quorum sensing systems regulate heterotrophic nitrification-aerobic denitrification by changing the activity of nitrogen-cycling enzymes. Environ Sci Ecotechnology 2020;2:100026.

[38] Humphries MD, Gurney K. Network 'small-world-ness': a quantitative method for determining canonical network equivalence. PLoS One 2008;3(4):e0002051.

[39] Tian L, Wang L. Multi-omics analysis reveals structure and function of biofilm microbial communities in a pre-denitrification biofilter. Sci Total Environ 2021;757:143908.

[40] Albertsen M, Hugenholtz P, Skarshewski A, Nielsen KL, Tyson GW, Nielsen PH. Genome sequences of rare, uncultured bacteria obtained by differential coverage binning of multiple metagenomes. Nat Biotechnol 2013;31(6):533-538.

661 **Figure Legends**

662 **Fig. 1** The concentration (left Y axis) and removal efficiency (right Y axis) of
663 wastewater nutrients and organic carbon during the *Tetrasphaera*-enriched microbiome
664 establishment process. (A) Orthophosphate (PO_4^{3-}-P), (B) Total organic carbon (TOC),
665 (C) Ammonia nitrogen (NH_4^+-N), and (D) Total nitrogen (TN).

666 **Fig. 2** The profiles of nutrient dynamics and removal efficiency of the *Tetrasphaera*-
667 enriched microbiome with different dosages of allylthiourea. Batch experiments were
668 set up to comparatively test the effects of 0, 1, and 5 mg/L of allylthiourea. (A) PO_4^{3-}-
669 P dynamics; (B) NH_4^+-N dynamics. (C) Removal efficiency of PO_4^{3-}-P and NH_4^+-N. (D)
670 DO dynamics.

671 **Fig. 3** Fluorescence *in situ* hybridization (FISH) and elemental distribution analyses of
672 full-scale WWTP sludge and lab-scale *Tetrasphaera*-enriched sludge. (A-B) FISH
673 images of local WWTP sludge collected on December 2nd, 2020 (A) and the
674 *Tetrasphaera*-enriched microbiome on day 143 (B). The colors denote stained bacterial
675 fractions in the community, with all bacteria in blue, *Ca.* Accumulibacter is yellow, and
676 *Tetrasphaera* is purple. (C) Elemental distribution and weight content (%) of
677 *Tetrasphaera*-rich sludge ash and WWTP sludge ash by scanning electron microscopy
678 and energy dispersive X-ray spectroscopy (SEM–EDS) analysis.

679 **Fig. 4** Microbial composition and dynamics during the establishment process of the
680 *Tetrasphaera*-enriched microbiome. (A) The top 20 bacteria at the genus level; (B) The
681 dynamic and phylogenetic analysis of the most abundant *Tetrasphaera*-related bacteria
682 (EBPR-ASV0001). The evolutionary history was inferred by the maximum likelihood
683 method and Kimura 2-parameter model. Two *Nitrosomonas europaea* sequences were
684 used as the outgroup. The global similarity of EBRP-ASV0001 compared with six
685 *Tetrasphaera* isolates is provided within the brackets.

686 **Fig. 5** Co-occurrence network of the *Tetrasphaera*-enriched microbiome-wide
687 associations based on pairwise Spearman's correlations between bacterial ASVs. Each
688 connection (i.e., edge) stands for a significant Spearman's correlation coefficient > 0.6
689 and a *P value* < 0.01. The size of each node is proportional to the number of connections
690 (i.e., degree), and the thickness of the edge is scaled according to the strengths of the
691 correlation between nodes. (A) Co-occurrence network colored by modularity class. (B)
692 Co-occurrence network colored by functionality. PAOs: *Tetrasphaera*, *Microlunatus*,
693 and *Gemmatimonas*; GAOs: *Micropruina*, *Kineosphaera*, and *Candidatus*
694 Competibacter; Nitrogen-removing bacteria: *Xanthobacter*, *Paracoccus*,
695 *Hyphomicrobium*, *Brevundimonas*, and *Bosea*.

696 **Fig. 6** Redundancy analysis (RDA) of (A) the nexus between the microbial community
697 and environmental variables and (B) the nexus between the microbial community and
698 EBPR performance. Four operational stages were defined based on the usage of
699 nitrification inhibitor allylthiourea during the microbiome establishment process: S1:
700 Natural enrichment phase (day 0-73) with no inhibitor; S2: Reinforced enrichment
701 phase (day 74-120) with 1 mg/L allylthiourea as inhibitor; S3: Transient shock phase
702 (day 121-127) with 5 mg/L allylthiourea as inhibitor); S4: Recovery phase (day 128-
703 170) with allylthiourea dosage adjusted back to 1 mg/L. The dashed arrow lines denote
704 two adjacent sampling time points in the first 73 days after reactor startup.

705

Figures

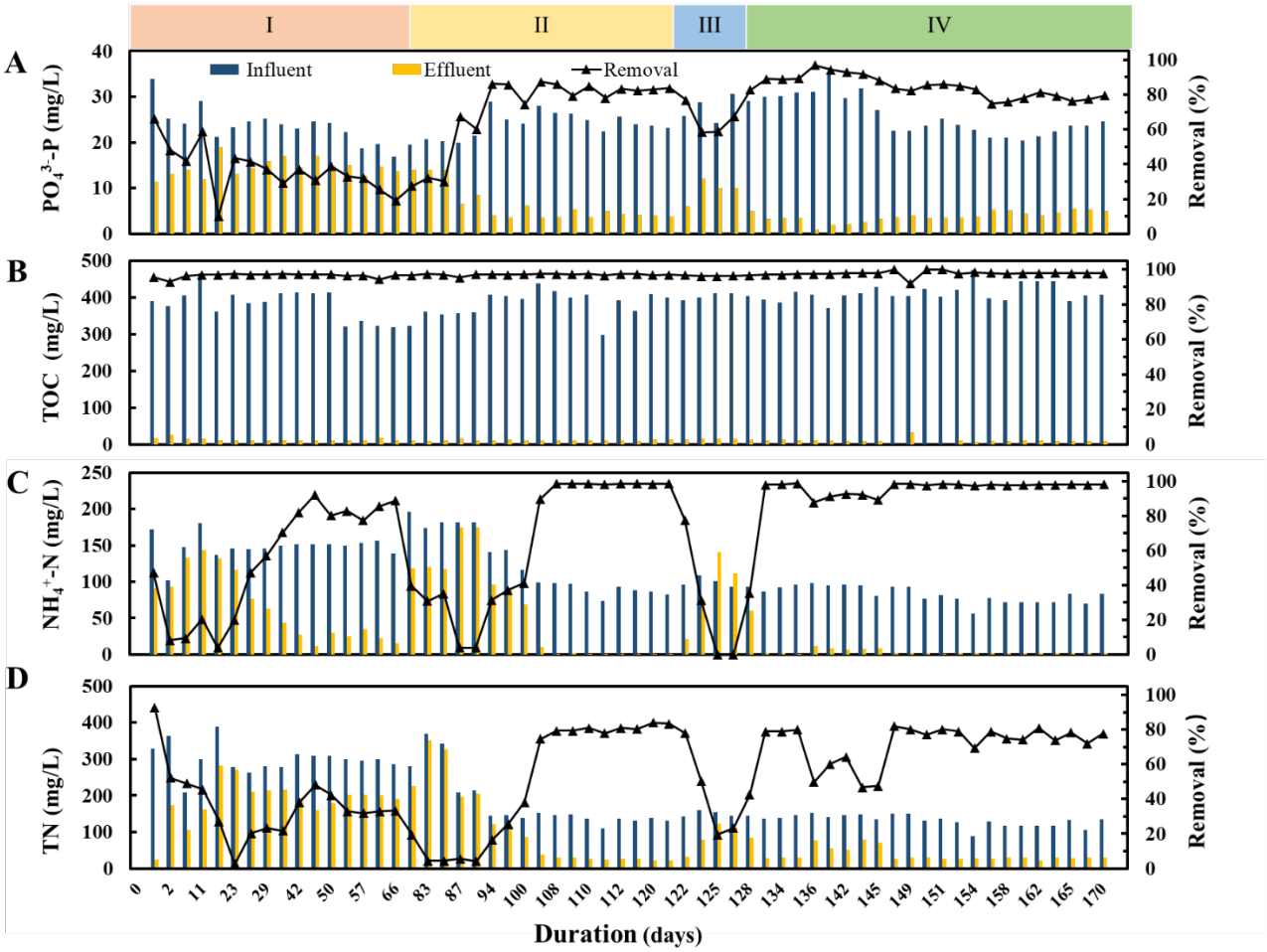

Fig. 1 The concentration (left Y axis) and removal efficiency (right Y axis) of wastewater nutrients and organic carbon during the *Tetrasphaera*-enriched microbiome establishment process. (A) Orthophosphate (PO_4^{3-}-P), (B) Total organic carbon (TOC), (C) Ammonia nitrogen (NH_4^+-N), and (D) Total nitrogen (TN).

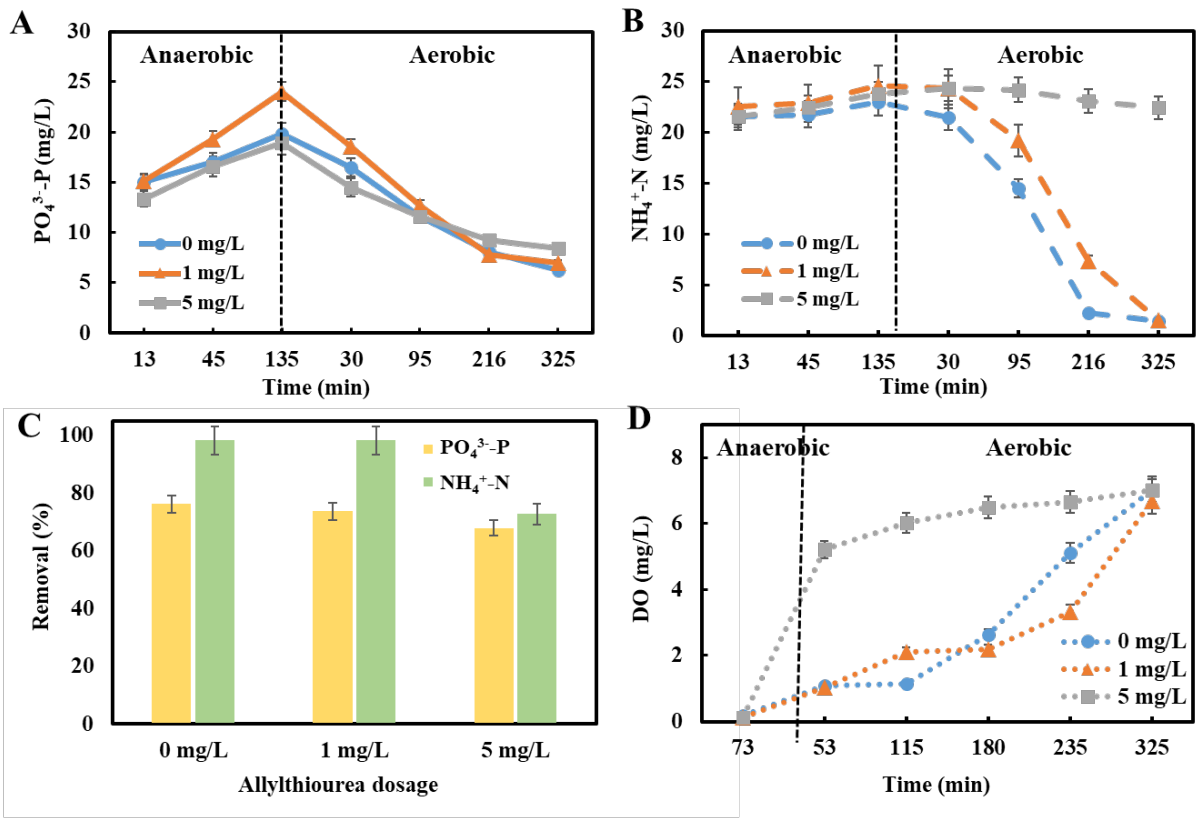

Fig. 2 The profiles of nutrient dynamics and removal efficiency of the *Tetrasphaera*-enriched microbiome with different dosages of allylthiourea. Batch experiments were set up to comparatively test the effects of 0, 1, and 5 mg/L of allylthiourea. (A) PO_4^{3-}-P dynamics; (B) NH_4^+-N dynamics. (C) Removal efficiency of PO_4^{3-}-P and NH_4^+-N. (D) DO dynamics.

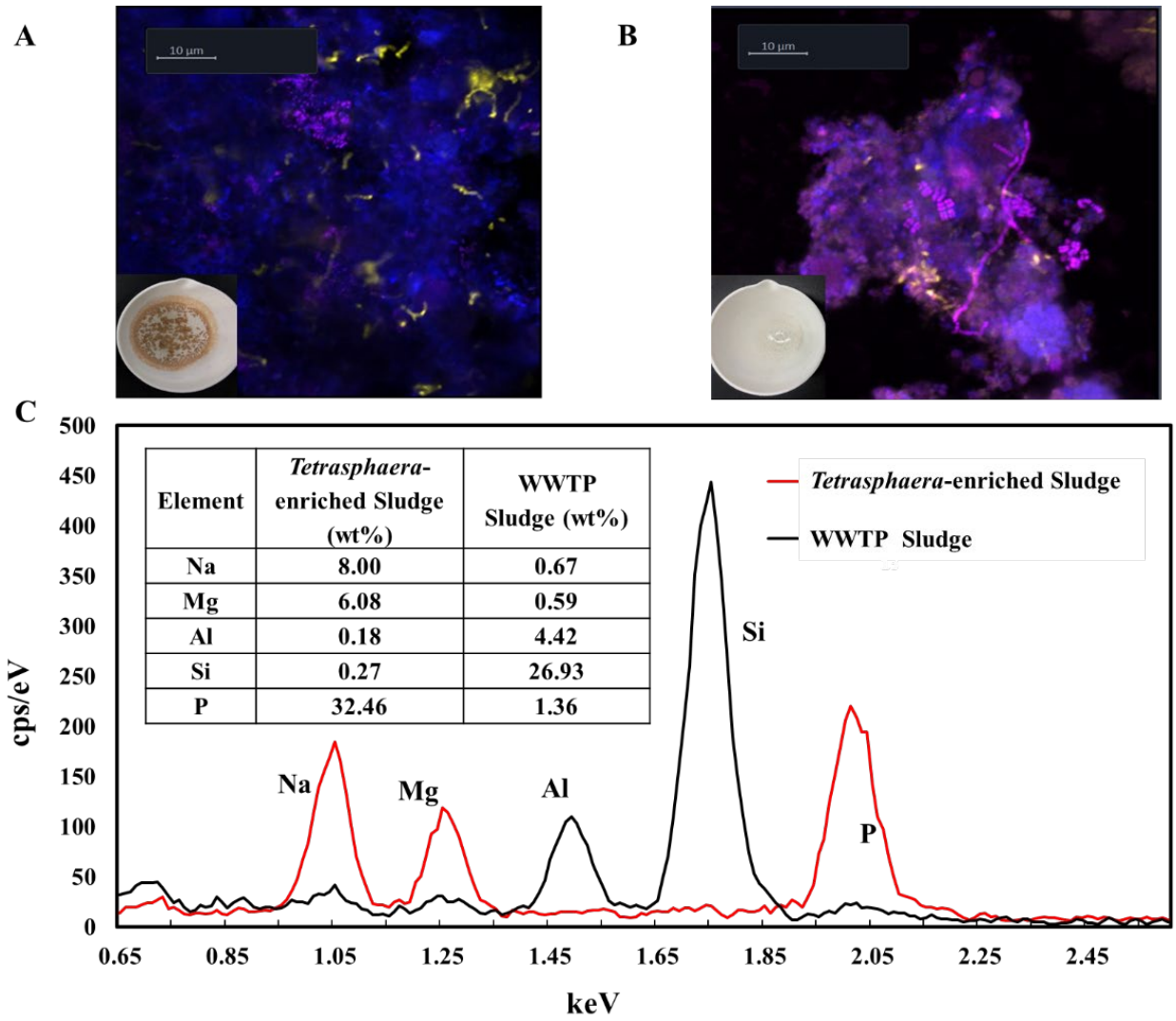

Element	*Tetrasphaera*-enriched Sludge (wt%)	WWTP Sludge (wt%)
Na	8.00	0.67
Mg	6.08	0.59
Al	0.18	4.42
Si	0.27	26.93
P	32.46	1.36

Fig. 3 Fluorescence *in situ* hybridization (FISH) and elemental distribution analyses of full-scale WWTP sludge and lab-scale *Tetrasphaera*-enriched sludge. (A-B) FISH images of local WWTP sludge collected on December 2nd, 2020 (A) and the *Tetrasphaera*-enriched microbiome on day 143 (B). The colors denote stained bacterial fractions in the community, with all bacteria in blue, *Ca.* Accumulibacter is yellow, and *Tetrasphaera* is purple. (C) Elemental distribution and weight content (%) of *Tetrasphaera*-rich sludge ash and WWTP sludge ash by scanning electron microscopy and energy dispersive X-ray spectroscopy (SEM–EDS) analysis.

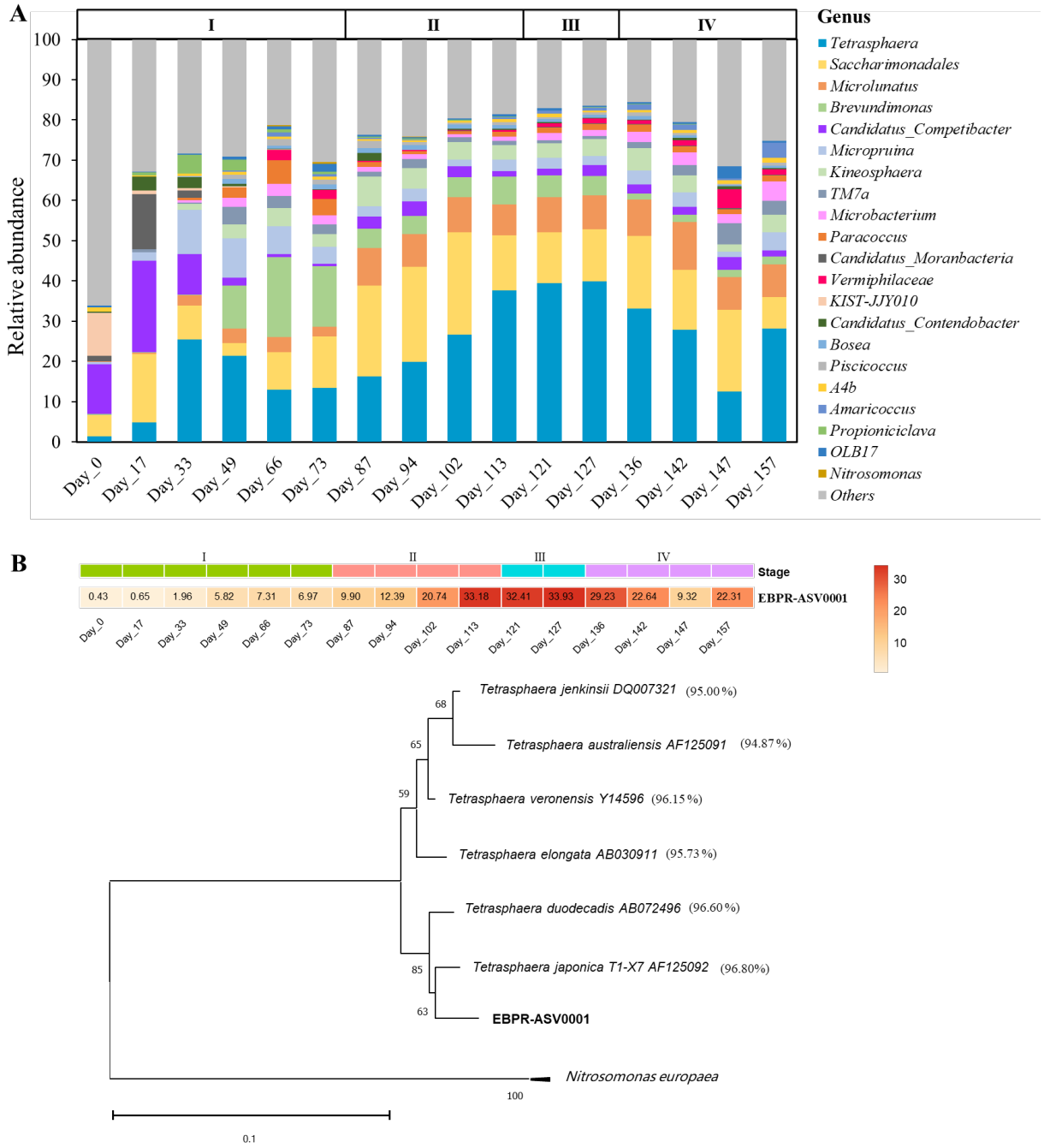

Fig. 4 Microbial composition and dynamics during the establishment process of the *Tetrasphaera*-enriched microbiome. (A) The top 20 bacteria at the genus level; (B) The dynamic and phylogenetic analysis of the most abundant *Tetrasphaera*-related bacteria (EBPR-ASV0001). The evolutionary history was inferred by the maximum likelihood method and Kimura 2-parameter model. Two *Nitrosomonas europaea* sequences were used as the outgroup. The global similarity of EBRP-ASV0001 compared with six *Tetrasphaera* isolates is provided within the brackets.

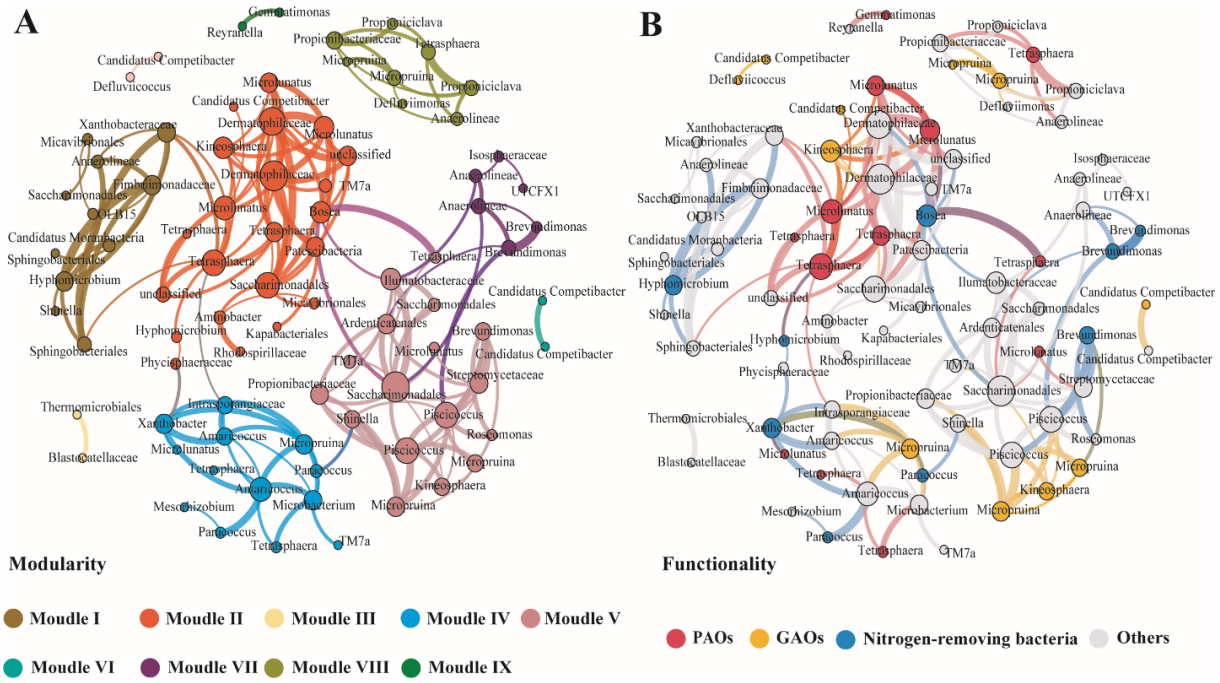

Fig. 5 Co-occurrence network of the *Tetrasphaera*-enriched microbiome-wide associations based on pairwise Spearman's correlations between bacterial ASVs. Each connection (i.e., edge) stands for a significant Spearman's correlation coefficient > 0.6 and a *P value* < 0.01. The size of each node is proportional to the number of connections (i.e., degree), and the thickness of the edge is scaled according to the strengths of the correlation between nodes. (A) Co-occurrence network colored by modularity class. (B) Co-occurrence network colored by functionality. PAOs: *Tetrasphaera*, *Microlunatus*, and *Gemmatimonas*; GAOs: *Micropruina*, *Kineosphaera*, and *Candidatus* Competibacter; Nitrogen-removing bacteria: *Xanthobacter*, *Paracoccus*, *Hyphomicrobium*, *Brevundimonas*, and *Bosea*.

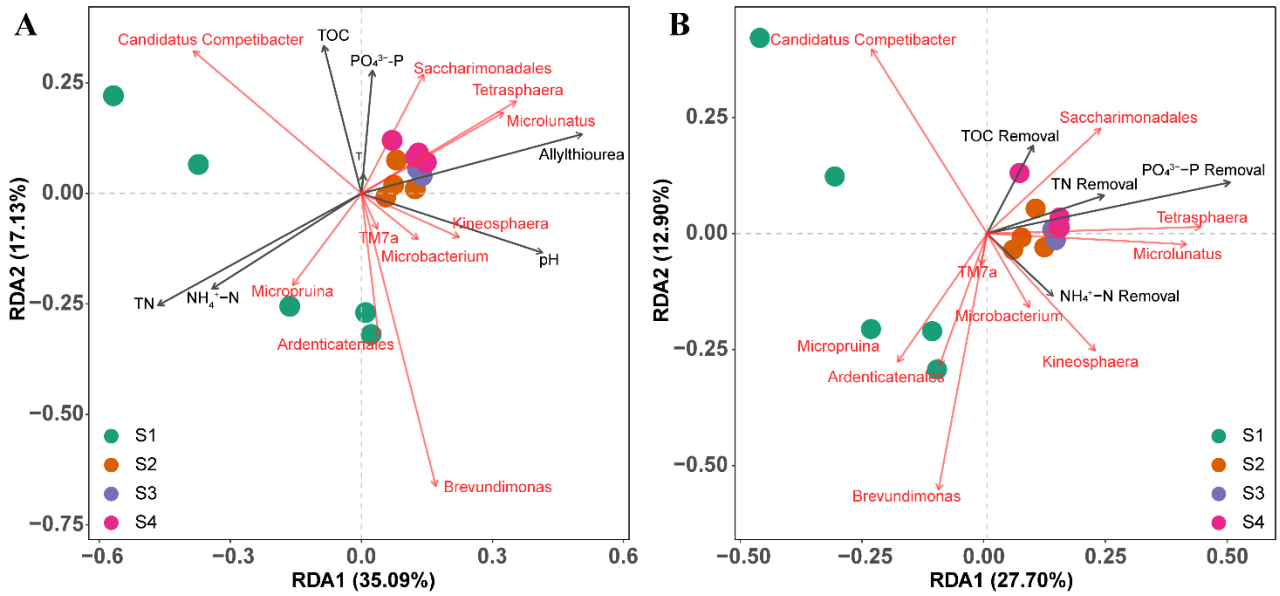

Fig. 6 Redundancy analysis (RDA) of (A) the nexus between the microbial community and environmental variables and (B) the nexus between the microbial community and EBPR performance. Four operational stages were defined based on the usage of nitrification inhibitor allylthiourea during the microbiome establishment process: S1: Natural enrichment phase (day 0-73) with no inhibitor; S2: Reinforced enrichment phase (day 74-120) with 1 mg/L allylthiourea as inhibitor; S3: Transient shock phase (day 121-127) with 5 mg/L allylthiourea as inhibitor); S4: Recovery phase (day 128-170) with allylthiourea dosage adjusted back to 1 mg/L. The dashed arrow lines denote two adjacent sampling time points in the first 73 days after reactor startup.